

# Residual-MPPI: Online Policy Customization for Continuous Control

Pengcheng Wang<sup>1\*</sup>, Chenran Li<sup>2\*</sup>, Catherine Weaver<sup>2</sup>, Kenta Kawamoto<sup>4</sup>, Masayoshi Tomizuka<sup>2</sup>,  
Chen Tang<sup>3†</sup>, and Wei Zhan<sup>2</sup>

<sup>1</sup>Xingjian College, Tsinghua University.

<sup>2</sup>Department of Mechanical Engineering, University of California, Berkeley.

<sup>3</sup>Department of Computer Science, University of Texas at Austin.

<sup>4</sup>Sony Research Inc., Japan.

\*wangpc20@mails.tsinghua.edu.cn, chenran\_li@berkeley.edu

†chen.tang@austin.utexas.edu

**Abstract:** Policies learned through Reinforcement Learning (RL) and Imitation Learning (IL) have demonstrated significant potential in achieving advanced performance in continuous control tasks. However, in real-world environments, it is often necessary to further customize a trained policy when there are additional requirements that were unforeseen during the original training phase. It is possible to fine-tune the policy to meet the new requirements, but this often requires collecting new data with the added requirements and access to the original training metric and policy parameters. In contrast, an online planning algorithm, if capable of meeting the additional requirements, can eliminate the necessity for extensive training phases and customize the policy without knowledge of the original training scheme or task. In this work, we propose a generic online planning algorithm for customizing continuous-control policies at the execution time which we call *Residual-MPPI*. It is able to customize a given prior policy on new performance metrics in few-shot and even zero-shot online settings. Also, Residual-MPPI only requires access to the action distribution produced by the prior policy, without additional knowledge regarding the original task. Through our experiments, we demonstrate that the proposed Residual-MPPI algorithm can accomplish the few-shot/zero-shot online policy customization task effectively, including customizing the champion-level racing agent, Gran Turismo Sophy (GT Sophy) 1.0, in the challenging car racing scenario, Gran Turismo Sport (GTS) environment. Demo videos are available on our website: <https://sites.google.com/view/residual-mppi>

**Keywords:** Policy customization, Combination of learning- and planning-based approaches, Model predictive control

## 1 Introduction

Policy learning algorithms such as Reinforcement Learning (RL) and Imitation Learning (IL) have been widely employed to synthesize parameterized control policies for a wide range of real-world motion planning and decision-making problems, such as navigation [1, 2], manipulation [3, 4, 5, 6] and locomotion [7, 8, 9]. In practice, real-world applications often impose additional requirements

---

\*Equal contribution

†Corresponding author

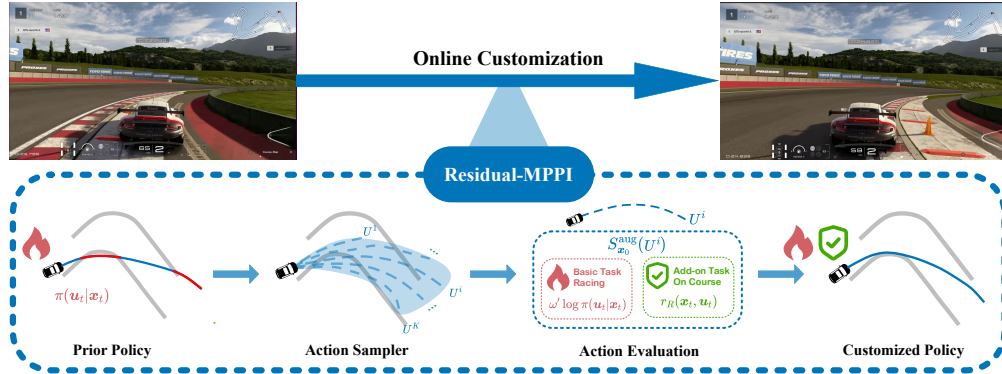


Figure 1: Overview of the proposed algorithm. In each planning loop, we utilize the prior policy to generate samples and then evaluate them through both the log likelihood of the prior policy and an add-on reward to obtain the customized actions. More details are in Sec. 3. In the experiments, we demonstrate that Residual-MPPI can accomplish the online policy customization task effectively, even in a challenging GTS environment with the champion-level racing agent, GT Sophy 1.0.

on the trained policies beyond those established during training, which can include novel goals [10], specific behavior preferences [11], and stringent safety criteria [12]. Retraining a new policy network whenever a new additional objective is encountered is both expensive and inefficient, as it may demand extensive training efforts. To enable the flexible deployment of embodied AI systems, it is thereby crucial to develop sample-efficient algorithms for synthesizing new policies that meet additional objectives while preserving the characteristics of the original policy [12, 13].

Recently, Li et al. [14] introduced a new problem setting termed *policy customization*, which provides a principled approach to address the aforementioned challenge. In policy customization, the objective is to develop a new policy given a prior policy, ensuring that the new policy: 1) retains the properties of the prior policy, and 2) fulfills additional requirements specified by a given downstream task. As an initial solution, the authors proposed the Residual Q-learning (RQL) framework. For discrete action spaces, RQL can leverage maximum-entropy Monte Carlo Tree Search [15] to customize the policy *online*, meaning at the execution time of the policy. In contrast, for continuous action spaces, RQL offers a solution based on Soft Actor-Critic (SAC) [16] to train a customized policy leveraging the prior policy before the real execution. While SAC-based RQL is more sample-efficient than training a new policy from scratch, the additional training steps that are required may still be expensive and time-consuming.

In this work, we propose *online policy customization for continuous action spaces* that eliminates the need for additional policy training. We leverage Model Predictive Path Integral (MPPI) [17], a sampling-based model predictive control (MPC) algorithm. Specifically, we propose *Residual-MPPI*, which integrates RQL into the MPPI framework, resulting in an online planning algorithm that customizes the prior policy at the execution time. The policy performance can be further enhanced by iteratively collecting data online to update the dynamics model. Our experiments in MuJoCo demonstrate that our method can effectively achieve zero-shot policy customization with a provided offline trained dynamics model. Furthermore, to investigate the scalability of our algorithm in complex environments, we evaluate Residual-MPPI in the challenging racing game environment, Gran Turismo Sport (GTS), in which we successfully customize the driving strategy of the champion-level racing agent, GT Sophy 1.0 [18], to adhere to additional safety constraints.

## 2 Preliminaries

In this section, we provide a concise introduction to two techniques that are used in our proposed algorithm: RQL and MPPI, to establish the foundations for the main technical results.

## 2.1 Policy Customization and Residual Q-Learning

We consider a discrete-time MDP problem defined by a tuple  $\mathcal{M} = (\mathcal{X}, \mathcal{U}, r, p)$ , where  $\mathcal{X} \subseteq \mathcal{R}^n$  is a continuous state space,  $\mathcal{U} \subseteq \mathcal{R}^m$  is a continuous action space,  $r : \mathcal{X} \times \mathcal{U} \rightarrow \mathbb{R}$  is the reward function, and  $p : \mathcal{X} \times \mathcal{U} \times \mathcal{X} \rightarrow [0, \infty)$  is the state transition probability density function. The prior policy  $\pi$  is fully trained as an optimal maximum-entropy policy to solve this MDP problem by performing the distribution of action  $\mathbf{u}_t$  with a given current state  $\mathbf{x}_t$ .

Meanwhile, the add-on task is specified by an add-on reward function  $r_R : \mathcal{X} \times \mathcal{U} \rightarrow \mathbb{R}$ . Therefore, the full task becomes a new MDP defined by a tuple  $\hat{\mathcal{M}} = (\mathcal{X}, \mathcal{U}, \omega r + r_R, p)$ , where the reward is defined as a weighted sum of the basic reward  $r$  and the add-on reward  $r_R$ . Thus, finding a policy that solves this new MDP accomplishes the policy customization task.

Li et al. [14] proposed the residual Q-learning framework to solve the policy customization task. Given the prior policy  $\pi$ , RQL is able to find this customized policy without knowledge of the prior reward  $r$ , which ensures broader applicability across different prior policies obtained through various methods, including those solely imitating demonstrations. In particular, as shown in their appendix [14], when we have access to the prior policy  $\pi$ , finding the maximum-entropy policy solving the full MDP problem  $\hat{\mathcal{M}} = (\mathcal{X}, \mathcal{U}, \omega r + r_R, p)$  is equivalent to solving an augmented MDP problem  $\mathcal{M}^{\text{aug}} = (\mathcal{X}, \mathcal{U}, \omega' \log \pi(\mathbf{u}|\mathbf{x}) + r_R, p)$ , where  $\omega'$  is a hyper-parameter that balances the optimality between original and add-on tasks.

## 2.2 Model Predictive Path Integral

Model Predictive Path Integral (MPPI) [17] is a sampling-based model predictive control (MPC) algorithm, which approximates the optimal solution of an (infinite-horizon) MDP through receding-horizon planning. MPPI evaluates the control inputs  $U = (\mathbf{u}_0, \mathbf{u}_1, \dots, \mathbf{u}_{T-1})$  with an accumulated reward function  $S_{\mathbf{x}_0}(U)$  defined by a reward function  $r$  and a terminal value estimator  $\phi$ :

$$S_{\mathbf{x}_0}(U) = \sum_{t=0}^{T-1} r(\mathbf{x}_t, \mathbf{u}_t) + \phi(\mathbf{x}_T), \quad (1)$$

where the intermediate state  $\mathbf{x}_t$  is calculated by recursively applying the transition dynamics on  $\mathbf{x}_0$ .

By applying an additive noise sequence  $\mathcal{E} = (\epsilon_0, \epsilon_1, \dots, \epsilon_{T-1})$  to a nominal control input sequence  $\hat{U}$ , MPPI obtains a disturbed control input sequence as  $U = \hat{U} + \mathcal{E}$  for subsequent optimization, where  $\mathcal{E}$  follows a multivariate Gaussian distribution with its probability density function defined as  $p(\mathcal{E}) = \prod_{t=0}^{T-1} ((2\pi)^m |\Sigma|)^{-\frac{1}{2}} \exp(-\frac{1}{2} \epsilon_t^T \Sigma^{-1} \epsilon_t)$ , where  $m$  is the dimension of the action space.

As shown by Williams et al. [17], the optimal action distribution that solves the MDP is

$$q^*(U) = \frac{1}{\eta} \exp\left(\frac{1}{\lambda} S_{\mathbf{x}_0}(U)\right) p(\mathcal{E}), \quad (2)$$

where  $\eta$  is the normalizing constant and  $\lambda$  is a positive scalar variable. MPPI approximates this distribution by assigning an importance sampling weight  $\omega(\mathcal{E}^k)$  to each noise sequence  $\mathcal{E}^k$  to update the nominal control input sequence.

$$\mathbf{u}_t = \hat{\mathbf{u}}_t + \sum_{k=1}^K \omega(\mathcal{E}^k) \epsilon_t^k, \quad (3)$$

where  $K$  is the number of samples, and  $\omega(\mathcal{E}^k)$  could be calculated as

$$\omega(\mathcal{E}^k) = \frac{1}{\mu} \left( S_{\mathbf{x}_0}(\hat{U} + \mathcal{E}^k) - \frac{\lambda}{2} \sum_{t=0}^{T-1} \hat{\mathbf{u}}_t^T \Sigma^{-1} (\hat{\mathbf{u}}_t + 2\epsilon_t^k) \right), \quad (4)$$

where  $\mu$  is the normalizing constant.

---

**Algorithm 1** Residual-MPPI

---

**Input:** Current state  $\mathbf{x}_0$ ; **Output:** Action Sequence  $\hat{U} = (\hat{\mathbf{u}}_0, \hat{\mathbf{u}}_1, \dots, \hat{\mathbf{u}}_{T-1})$ .  
**Require:** Dynamics of the system  $F$ ; Number of samples  $K$ ; Planning horizon  $T$ ; Prior policy  $\pi$ ;  
Disturbance covariance matrix  $\Sigma$ ; Add-on reward  $r_R$ ; Temperature scalar  $\lambda$

- 1: **for**  $t = 0, \dots, T - 1$  **do** ▷ Initialize the action sequence from the prior policy
- 2:      $\hat{\mathbf{u}}_t \leftarrow \arg \max \pi(\mathbf{u}_t | \mathbf{x}_t)$
- 3:      $\mathbf{x}_{t+1} \leftarrow F(\mathbf{x}_t, \hat{\mathbf{u}}_t)$
- 4: **end for**
- 5: **for**  $k = 1, \dots, K$  **do** ▷ Evaluate the sampled action sequence
- 6:     Sample noise  $\mathcal{E}^k = \{\epsilon_0^k, \epsilon_1^k, \dots, \epsilon_{T-1}^k\}$
- 7:     **for**  $t = 0, \dots, T - 1$  **do**
- 8:          $\mathbf{x}_{t+1} \leftarrow F(\mathbf{x}_t, \hat{\mathbf{u}}_t + \epsilon_t^k)$
- 9:          $S(\mathcal{E}^k)_+ = \gamma^t \times (r_R(\mathbf{x}_t, \hat{\mathbf{u}}_t + \epsilon_t^k) + \omega' \log \pi(\hat{\mathbf{u}}_t + \epsilon_t^k | \mathbf{x}_t)) - \lambda \hat{\mathbf{u}}_t^T \Sigma^{-1} \epsilon_t^k$
- 10:     **end for**
- 11: **end for**
- 12:  $\beta = \min_k S(\mathcal{E}^k)$  ▷ Update the action sequence
- 13:  $\eta \leftarrow \sum_{k=1}^K \exp\left(\frac{1}{\lambda} (S(\mathcal{E}^k) - \beta)\right)$
- 14: **for**  $k = 1, \dots, K$  **do**
- 15:      $\omega(\mathcal{E}^k) \leftarrow \frac{1}{\eta} \exp\left(\frac{1}{\lambda} (S(\mathcal{E}^k) - \beta)\right)$
- 16: **end for**
- 17: **for**  $t = 0, \dots, T - 1$  **do**
- 18:      $\hat{\mathbf{u}}_{t+1} = \sum_{k=1}^K \omega(\mathcal{E}^k) \epsilon_t^k$
- 19: **end for**
- 20: **return**  $U$

---

### 3 Method

Our objective is to address the policy customization challenge under the online setting for general continuous control problems. We aim to leverage a pre-trained prior policy  $\pi$ , along with a dynamics model  $F$ , to approximate the optimal solution to the augmented MDP problem  $\mathcal{M}^{\text{aug}}$ , in an online manner. To address this problem, we propose a novel algorithm, *Residual Model Predictive Path Integral* (Residual-MPPI), which is broadly applicable to any maximum-entropy prior policy with a dynamics model of the environment. The proposed algorithm is summarized in Algorithm 1 and Figure 1. In this section, we first establish the theoretical foundation of our approach by verifying the maximum-entropy property of MPPI. We then refine the MPPI method with the derived formulation to approximate the solution of the  $\mathcal{M}^{\text{aug}}$ . Lastly, we discuss the dynamics learning and fine-tuning method used in our implementation.

#### 3.1 Residual-MPPI

MPPI is a widely used sampling-based MPC algorithm that has demonstrated promising results in various continuous control tasks. To achieve online policy customization, i.e. solving the augmented MDP  $\mathcal{M}^{\text{aug}}$  efficiently during online execution, we utilize MPPI as the foundation of our algorithm.

As shown in the preliminary, RQL requires the planning algorithm to comply with the principle of maximum entropy. To validate that MPPI adheres to the principle of maximum-entropy, we note the Theorem 1 where a step-by-step breakdown proof can be found in Appendix A

**Theorem 1.** *Given an MDP defined by  $\mathcal{M} = (\mathcal{X}, \mathcal{U}, r, p)$ , with a deterministic state transition  $p$  defined with respect to a dynamics model  $F$  and a discount factor  $\gamma = 1$ , the distribution of the action sequence  $q^*(U)$  at state  $\mathbf{x}_0$  in horizon  $T$ , where each action  $\mathbf{u}_t, t = 0, \dots, T - 1$  is sequentially sampled from the maximum-entropy policy [19] with an entropy weight  $\alpha$  is*

$$q^*(U) = \frac{1}{Z_{\mathbf{x}_0}} \exp\left(\frac{1}{\alpha} \left(\sum_{t=0}^{T-1} r(\mathbf{x}_t, \mathbf{u}_t) + V^*(\mathbf{x}_T)\right)\right), \quad (5)$$

where  $V^*$  is the soft value function [19] and  $\mathbf{x}_t$  is defined recursively from  $\mathbf{x}_0$  and  $U$  through the dynamics model  $F$  as  $\mathbf{x}_{t+1} = F(\mathbf{x}_t, \mathbf{u}_t)$ ,  $t = 0, \dots, T - 1$ .

If we have  $\lambda = \alpha$  and let  $V^*$  as the terminal value estimator, The distribution in Eq. (5) is equivalent to the one in Eq. (2), that is the optimal distribution that MPPI tries to approximate, but under the condition that the  $p(\mathcal{E})$  is a Gaussian distribution with infinite variance, i.e. a uniform distribution. It suggests that MPPI can well approximate the maximum-entropy optimal policy with a discount factor  $\gamma$  close to 1 and a large noise variance. We can then derive Residual-MPPI straightforwardly by defining the evaluation function  $S_{\mathbf{x}_0}(U)$  in MPPI as

$$S_{\mathbf{x}_0}^{\text{aug}}(U) = \sum_{t=0}^{T-1} \gamma^t \cdot (r_R(\mathbf{x}_t, \mathbf{u}_t) + \omega' \log \pi(\mathbf{u}_t | \mathbf{x}_t)), \quad (6)$$

to solve the  $\mathcal{M}^{\text{aug}}$ , therefore approximates the optimal customized policy online.

Additionally, the performance and sample-efficiency of MPPI depend on the approach to initialize the nominal input sequence  $\hat{U}$ . In our context, the prior policy serves as a natural source for initializing the nominal control inputs. As shown at line 1 in Algorithm 1, by recursively applying the prior policy and the dynamics, we could initialize a nominal trajectory with a tunable exploration noise to construct a Gaussian prior distribution for sampling. During implementation and experiments, we found that using the nominal action sequence itself as a candidate sequence for evaluation can effectively increase sampling stability.

### 3.2 Dynamics Learning and Fine-tuning

In scenarios where an effective dynamics model is unavailable in a prior, it is necessary to develop a learned dynamics model. To this end, we established a dynamics training pipeline utilizing the prior policy for data collection. In our implementation, we employed three main techniques to enhance the model’s capacity for accurately predicting environmental states as follows:

**Multi-step Error:** The prediction errors of an imperfect dynamics model accumulate over time steps. In the worst case, compounding multi-step errors can grow exponentially [20]. To ensure the accuracy of the dynamics model over the long term, we use a multi-step error  $\sum_{t=0}^T \gamma^t \times (s_t - \hat{s}_t)^2$  as the loss function for dynamics training, where  $s_t$  and  $\hat{s}_t$  are the ground-truth and predicted state.

**Exploration Noise:** The prior policy’s behavior sticks around the optimal behavior to the prior task, which means the roll-out samples collected using the prior policy concentrated to a limited region in the state space. It limits the generalization performance of the dynamics model under the policy customization setting. Therefore, during the sampling process, we add Gaussian exploration noises to the prior policy actions to enhance sample diversity.

**Fine-tuning with Online Data:** Since the residual-MPPI planner solves the customized task objective, its behavior is different from the prior policy. Thus, the residual-MPPI planner may encounter states that are not contained in the dynamics training dataset collected using the prior policy. Therefore, the learned dynamics model could be inaccurate on these unseen states. In this case, we can follow the common model-based RL routine to iteratively collect data using the residual-MPPI planner and update the dynamics model using the collected in-distribution data.

## 4 MuJoCo Experiments

In this section, we evaluate the performance of the proposed algorithms in different environments selected from MuJoCo [21]. In Sec. 4.1, we provide the configurations of our experiments, including the settings of policy customization tasks in different environments, baselines, and evaluation metrics. In Sec. 4.2, we present and analyze the experimental results. Please refer to the appendices for detailed experiment configurations, implementations, and visualizations.

Table 1: Experimental Results of Zero-shot Residual-MPPI in MuJoCo

Env.	Policy	Full Task	Basic Task	Add-on Task	
		Total Reward	Basic Reward	$ \bar{\theta} $	Add-on Reward
Half Cheetah	Prior Policy	1004.79 $\pm$ 38.88	2452.30 $\pm$ 23.55	0.14 $\pm$ 0.00	-1447.50 $\pm$ 31.29
	Full-MPPI	-3590.68 $\pm$ 315.50	-1172.52 $\pm$ 142.35	0.24 $\pm$ 0.03	-2418.16 $\pm$ 314.14
	Guided-MPPI	1821.19 $\pm$ 285.44	2137.76 $\pm$ 179.70	0.03 $\pm$ 0.01	-316.57 $\pm$ 108.01
	Residual-MPPI	<b>1948.14 <math>\pm</math> 34.56</b>	2189.45 $\pm$ 28.87	<b>0.02 <math>\pm</math> 0.00</b>	<b>-241.31 <math>\pm</math> 28.86</b>
Env.	Policy	Total Reward	Basic Reward	$ \bar{\theta} $	Add-on Reward
Swimmer	Prior Policy	-245.01 $\pm$ 5.95	346.24 $\pm$ 3.44	0.59 $\pm$ 0.01	-591.24 $\pm$ 6.40
	Full-MPPI	-1677.68 $\pm$ 124.86	13.46 $\pm$ 6.27	1.69 $\pm$ 0.12	-1691.13 $\pm$ 124.17
	Guided-MPPI	-147.77 $\pm$ 5.54	294.28 $\pm$ 3.87	0.44 $\pm$ 0.01	-442.05 $\pm$ 7.61
	Residual-MPPI	<b>-61.00 <math>\pm</math> 5.20</b>	276.21 $\pm$ 3.49	<b>0.34 <math>\pm</math> 0.01</b>	<b>-337.21 <math>\pm</math> 7.67</b>
Env.	Policy	Total Reward	Basic Reward	$\bar{z}$	Add-on Reward
Hopper	Prior Policy	7250.67 $\pm$ 49.39	3575.02 $\pm$ 9.35	1.37 $\pm$ 0.00	3675.02 $\pm$ 48.21
	Full-MPPI	21.09 $\pm$ 3.52	3.72 $\pm$ 0.81	1.24 $\pm$ 0.00	17.37 $\pm$ 2.93
	Guided-MPPI	6146.35 $\pm$ 1605.06	3073.04 $\pm$ 682.71	1.36 $\pm$ 0.03	3073.31 $\pm$ 927.26
	Residual-MPPI	<b>7398.29 <math>\pm</math> 103.92</b>	3560.97 $\pm$ 19.04	<b>1.38 <math>\pm</math> 0.01</b>	<b>3837.32 <math>\pm</math> 105.61</b>
Env.	Policy	Total Reward	Basic Reward	$\bar{v}_y$	Add-on Reward
Ant	Prior Policy	6299.17 $\pm$ 957.16	6133.41 $\pm$ 891.45	0.17 $\pm$ 0.22	165.76 $\pm$ 221.35
	Full-MPPI	-2792.20 $\pm$ 154.94	-2779.91 $\pm$ 120.28	-0.01 $\pm$ 0.08	-12.29 $\pm$ 87.81
	Guided-MPPI	5485.85 $\pm$ 1773.90	5277.66 $\pm$ 1670.04	0.21 $\pm$ 0.26	208.19 $\pm$ 260.70
	Residual-MPPI	<b>6808.38 <math>\pm</math> 599.48</b>	5969.61 $\pm$ 490.13	<b>0.84 <math>\pm</math> 0.20</b>	<b>838.77 <math>\pm</math> 198.08</b>

The evaluation results are computed over 500 episodes with all methods. The results are in the form of mean  $\pm$  std.

## 4.1 Experiment Setup

**Environments.** In each environment, we design the basic and add-on rewards to illustrate a practical application scenario, where the basic reward corresponds to some basic task requirements and the add-on reward reflects customized specifications such as behavior preference or additional task objectives. The detailed configurations of the environments can be found in Appendix B.1.

**Baselines.** In our experiments, we mainly compare the performance of the proposed residual-MPPI algorithm against three baselines:

- **Prior Policy:** We utilize SAC to train the prior policy on the basic task for policy customization. At test time, we evaluate its performance on the overall task without customization, which serves as a baseline to show the effectiveness of the proposed algorithm.
- **Guided-MPPI:** We introduced Guided-MPPI from the idea proposed in the literature [10, 22] that leverages the prior policy to guide planning. The samples are obtained from the same prior policy used in Residual-MPPI. Note that Guided-MPPI utilizes the unbiased ground truth reward (i.e.,  $\omega r + r_R$ ). By comparing Residual-MPPI against Guided-MPPI, we aim to validate the necessity of Residual-MPPI under this ideal setting.
- **Full-MPPI:** Additionally, we apply the MPPI with no prior on the MDP problem of the full task (i.e.,  $\omega r + r_R$ ). We aim to compare Residual-MPPI against it to validate that our proposed algorithm can effectively leverage the prior policy to boost online planning.

**Metric.** We aim to validate a policy’s performance from two perspectives: 1) whether the policy is customized toward the add-on reward; 2) whether the customized policy still maintains the same level of performance on the basic task. Therefore, we use the average basic reward as the metric to evaluate a policy’s performance on the basic task. Meanwhile, we use the average add-on reward and task-specific metrics as the metrics for evaluating a policy’s performance for the customized objective. Furthermore, we use the total reward to evaluate the joint optimality of the solved policy.

## 4.2 Results and Discussions

The experimental results, summarized in Table 1, demonstrate the effectiveness of Residual-MPPI for online policy customization. Across all the tested environments, the customized policies achieve significant improvements over the prior policies in meeting the objectives of the add-on tasks. Simultaneously, these customized policies maintain a similar level of performance as the prior policies on the basic tasks. In comparing the performance with baseline approaches, it is evident that the Guided-MPPI policies, despite utilizing the same sampling strategy and having full access to the rewards of both basic and add-on tasks, underperform in all environments relative to the proposed Residual-MPPI. Furthermore, the Full-MPPI policies, which also have the full reward information, fail in all tasks. This outcome highlights a prevalent challenge in planning-based methods: effective planning necessitates ample samples and a sufficiently long planning horizon or an accurate terminal value estimator to correctly evaluate the optimality of actions. While Guided-MPPI improves the estimation of optimal actions through more efficient sampling, it remains hindered by its limited ability to account for the long-term impacts of actions within finite planning horizons. In contrast, Residual-MPPI implicitly inherits the original task reward through the prior policy log likelihood, which is informed by the Q functions optimized over an infinite horizon or demonstrations.

## 5 Customizing Champion-level Autonomous Racing Policy

With the effective results in standard benchmark environments, we are further interested in whether the proposed algorithm can be applied to effectively customize an advanced policy for a more sophisticated continuous control task. Gran Turismo Sport (GTS) is a realistic racing simulator with high-fidelity vehicle dynamics. GT Sophy 1.0 [18], a DRL-based racing policy, has shown to outperform the world’s best drivers among the global players. To further investigate the scalability of our algorithm and its robustness when dealing with more complex environments and advanced policies, we carried out further customization experiments on GT Sophy 1.0 in the GTS environment.

### 5.1 Experiment Setup

Though GT Sophy 1.0 is a highly advanced system with superhuman racing skills, it tends to exhibit too aggressive route selection as the well-trained policy has the ability to keep stable on the simulated grass. However, in real-world racing, such behaviors would be considered dangerous and fragile because of the time-varying physical properties of real grass surfaces and tires. Therefore, we establish the task as customizing the policy to a safer route selection. Formally, the customization goal is to help the GT Sophy 1.0 drive *on course* while maintaining its superior racing performance. This kind of customization objective could potentially be used to foster robust sim-to-real transfer of agile control policies for many related problem domains.

Notably, GTS runs on an independent PS5 platform with a fixed running frequency of 60Hz, which imposes real-time requirements for online control, making it closer to real-world settings. As the dynamics model is not available in a prior, we adopt a simple MLP architecture to design a dynamics model and train it using the techniques introduced in Sec. 3.2. The configurations of the environments and implementation details can be found in Appendix C.

As the pre-trained GT Sophy 1.0 policy is constructed with complex rewards and regulations, we leverage the average lap time and number of off-course steps as the metrics. In addition to zero-shot Residual-MPPI, we also evaluate a few-shot version of our algorithm, in which we iteratively update the dynamics with the customized planner’s trajectories to further improve the performance. We also consider Residual-SAC [14] as another baseline to validate the advantage of online Residual-MPPI against RL-based solutions in the challenging racing problem.

Table 2: Experimental Results of Residual-MPPI in GTS

Policy	GT Sophy 1.0	Zero-shot MPPI	Few-shot MPPI	Residual-SAC
Lap Time	117.77 $\pm$ 0.08	121.99 $\pm$ 0.57	<b>120.75 <math>\pm</math> 0.37</b>	130.00 $\pm$ 0.13
Off-course Steps	93.13 $\pm$ 1.98	43.53 $\pm$ 7.40	<b>36.60 <math>\pm</math> 6.04</b>	0.87 $\pm$ 0.78

The evaluation results are computed over 30 laps with all methods.

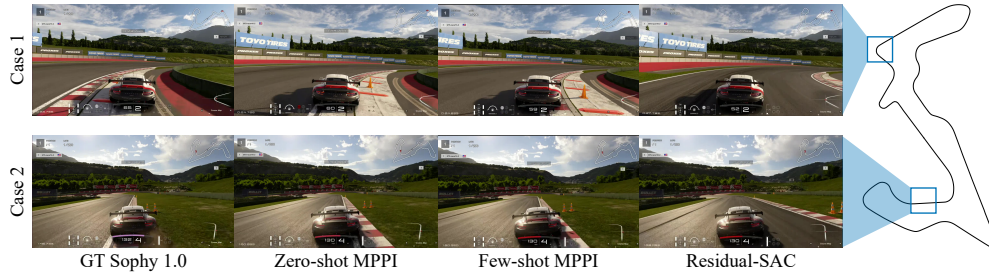


Figure 2: Typical Route Selection of Policies

## 5.2 Results and Discussions

The experimental results, summarized in Table 2, demonstrate that Residual-MPPI significantly enhances the safety of GT Sophy 1.0 by reducing its off-course steps, albeit with a marginal increase in lap time. Further improvements are observed after employing data gathered during the customization process to fine-tune the dynamics under a few-shot setting. This few-shot version of Residual-MPPI outperforms the zero-shot version in terms of lap time and off-course steps. Though the customized policies can not eliminate all the off-course cases, it is worth noting that these cases are significantly less severe than those in GT Sophy 1.0. The average and maximum off-course distance of GT Sophy 1.0 in a typical run is 0.69m and 3.21m, while for Few-shot Residual-MPPI are 0.37m and 1.13m.

In contrast, Residual-SAC yields a very conservative customized policy. As shown in Figure 2, it is obvious that the Residual-SAC policy behaves sub-optimally and overly yields to the on-course constraints. It is worth noting that over *80,000 laps* of roll-outs are collected to achieve the current performance of Residual-SAC. In contrast, the data used to train GTS dynamics for Residual-MPPI, along with the online data for dynamics model fine-tuning, amounted to only approximately *2,000* and *100* laps respectively. As discussed in safe RL and curriculum learning methods [23, 24], when training with constraints, it is easy for RL to yield to an overly conservative behavior.

## 6 Related Works

In this section, we provide a concise introduction to the related works of the proposed method. Please refer to the appendices for detailed discussion. Here we briefly discuss the literature in three topics: 1) *Model-based RL*: Many works focused on combining learning-based agents with classical planning methods to enhance performance, especially in various model-based RL approaches [25, 26]. However, those methods mainly address the planning within the same task and have full reward information of it. As for policy customization, it requires jointly optimizing both the original task of the prior policy without access to the reward information and add-on tasks, which makes it unsolvable by these methods. 2) *Planning with Prior Policy*: Some work in the literature address the similar customization requirements of the pre-trained prior policy [10, 14, 22]. Li et al. [22] consider modeling the reward with hand-designed features, which introduce further bias and constrain the overall performance. Rhinehart et al. [10] formulate the additional requirements as goals, which are not flexible to specify. Residual-MCTS [14] applies to discretized action, which makes it difficult to extend to continuous and more complex tasks. 3) *RL Fine-tuning*: There have been numerous



works considering the topic of fine-tuning policies [27, 28, 29, 30]. However, these methods still require additional training for each new customization goal, which hinders flexible deployment.

## 7 Limitations and Future Work

**Prior Policy and Dynamics:** Currently, Residual-MPPI is *bottlenecked* by the prior policy and dynamics. The proposed algorithm requires its prior policy to accurately indicate the desired behavior respect to the original task. Policies without careful modeling or sufficient training could mislead the evaluation step of the proposed algorithm and result in poor planning outcomes. Also, the proposed algorithm relies on an accurate dynamics model to correctly rollout the states. In the future, we can introduce more advanced methods in policies and dynamics training, such as diffusion policies [31, 32, 33] and world models [34, 35], to improve the prior policies and dynamics.

**Terminal Value Estimation:** Similar to most online planning methods, our algorithm also needs a sufficiently long horizon to reduce the error brought by the absence of a terminal value estimator. Though utilizing prior policy partially addresses the problem as we discussed in Sec. 4.2, it can not fully eliminate the error. Techniques like Jump-start RL [27] and RL-driven MPPI [36] could be incorporated in the proposed framework in the few-shot setting by using the collected data to learn a Residual Q-function online as a terminal value estimator, which will be one of our future works.

## References

- [1] P. Mirowski, R. Pascanu, F. Viola, H. Soyer, A. J. Ballard, A. Banino, M. Denil, R. Goroshin, L. Sifre, K. Kavukcuoglu, et al. Learning to navigate in complex environments. *arXiv preprint arXiv:1611.03673*, 2016.
- [2] A. Francis, A. Faust, H.-T. L. Chiang, J. Hsu, J. C. Kew, M. Fiser, and T.-W. E. Lee. Long-range indoor navigation with prm-rl. *IEEE Transactions on Robotics*, 36(4):1115–1134, 2020.
- [3] O. M. Andrychowicz, B. Baker, M. Chociej, R. Jozefowicz, B. McGrew, J. Pachocki, A. Petron, M. Plappert, G. Powell, A. Ray, et al. Learning dexterous in-hand manipulation. *The International Journal of Robotics Research*, 39(1):3–20, 2020.
- [4] T. Zhang, Z. McCarthy, O. Jow, D. Lee, X. Chen, K. Goldberg, and P. Abbeel. Deep imitation learning for complex manipulation tasks from virtual reality teleoperation. In *2018 IEEE international conference on robotics and automation (ICRA)*, pages 5628–5635. IEEE, 2018.
- [5] A. Mandlekar, D. Xu, J. Wong, S. Nasiriany, C. Wang, R. Kulkarni, L. Fei-Fei, S. Savarese, Y. Zhu, and R. Martín-Martín. What matters in learning from offline human demonstrations for robot manipulation. *arXiv preprint arXiv:2108.03298*, 2021.
- [6] A. Rajeswaran, V. Kumar, A. Gupta, G. Vezzani, J. Schulman, E. Todorov, and S. Levine. Learning complex dexterous manipulation with deep reinforcement learning and demonstrations. *arXiv preprint arXiv:1709.10087*, 2017.
- [7] X. B. Peng and M. Van De Panne. Learning locomotion skills using deeprl: Does the choice of action space matter? In *Proceedings of the ACM SIGGRAPH/Eurographics Symposium on Computer Animation*, pages 1–13, 2017.
- [8] X. B. Peng and M. Van De Panne. Learning locomotion skills using deeprl: Does the choice of action space matter? In *Proceedings of the ACM SIGGRAPH/Eurographics Symposium on Computer Animation*, pages 1–13, 2017.
- [9] S. Gangapurwala, M. Geisert, R. Orsolino, M. Fallon, and I. Havoutis. Rloc: Terrain-aware legged locomotion using reinforcement learning and optimal control. *IEEE Transactions on Robotics*, 38(5):2908–2927, 2022.
- [10] N. Rhinehart, R. McAllister, and S. Levine. Deep imitative models for flexible inference, planning, and control. *arXiv preprint arXiv:1810.06544*, 2018.
- [11] D. M. Ziegler, N. Stiennon, J. Wu, T. B. Brown, A. Radford, D. Amodei, P. Christiano, and G. Irving. Fine-tuning language models from human preferences. *arXiv preprint arXiv:1909.08593*, 2019.
- [12] Y. Lu, J. Fu, G. Tucker, X. Pan, E. Bronstein, R. Roelofs, B. Sapp, B. White, A. Faust, S. Whiteson, et al. Imitation is not enough: Robustifying imitation with reinforcement learning for challenging driving scenarios. In *2023 IEEE/RSJ International Conference on Intelligent Robots and Systems (IROS)*, pages 7553–7560. IEEE, 2023.
- [13] M. Harmel, A. Paras, A. Pasternak, and G. Linscott. Scaling is all you need: Training strong policies for autonomous driving with jax-accelerated reinforcement learning. *arXiv preprint arXiv:2312.15122*, 2023.
- [14] C. Li, C. Tang, H. Nishimura, J. Mercat, M. Tomizuka, and W. Zhan. Residual q-learning: Offline and online policy customization without value. *Advances in Neural Information Processing Systems*, 36, 2024.
- [15] C. Xiao, R. Huang, J. Mei, D. Schuurmans, and M. Müller. Maximum entropy monte-carlo planning. *Advances in Neural Information Processing Systems*, 32, 2019.

- [16] T. Haarnoja, A. Zhou, P. Abbeel, and S. Levine. Soft actor-critic: Off-policy maximum entropy deep reinforcement learning with a stochastic actor. In *International conference on machine learning*, pages 1861–1870. PMLR, 2018.
- [17] G. Williams, N. Wagener, B. Goldfain, P. Drews, J. M. Rehg, B. Boots, and E. A. Theodorou. Information theoretic mpc for model-based reinforcement learning. In *2017 IEEE international conference on robotics and automation (ICRA)*, pages 1714–1721. IEEE, 2017.
- [18] P. R. Wurman, S. Barrett, K. Kawamoto, J. MacGlashan, K. Subramanian, T. J. Walsh, R. Capobianco, A. Devlic, F. Eckert, F. Fuchs, et al. Outracing champion gran turismo drivers with deep reinforcement learning. *Nature*, 602(7896):223–228, 2022.
- [19] T. Haarnoja, H. Tang, P. Abbeel, and S. Levine. Reinforcement learning with deep energy-based policies. In *International conference on machine learning*, pages 1352–1361. PMLR, 2017.
- [20] A. Venkatraman, M. Hebert, and J. Bagnell. Improving multi-step prediction of learned time series models. In *Proceedings of the AAAI Conference on Artificial Intelligence*, volume 29, 2015.
- [21] E. Todorov, T. Erez, and Y. Tassa. Mujoco: A physics engine for model-based control. In *2012 IEEE/RSJ International Conference on Intelligent Robots and Systems*, pages 5026–5033, 2012. doi:10.1109/IROS.2012.6386109.
- [22] C. Li, T. Trinh, L. Wang, C. Liu, M. Tomizuka, and W. Zhan. Efficient game-theoretic planning with prediction heuristic for socially-compliant autonomous driving. *IEEE Robotics and Automation Letters*, 7(4):10248–10255, 2022.
- [23] S. Mo, X. Pei, and C. Wu. Safe reinforcement learning for autonomous vehicle using monte carlo tree search. *IEEE Transactions on Intelligent Transportation Systems*, 23(7):6766–6773, 2021.
- [24] L. Anzalone, P. Barra, S. Barra, A. Castiglione, and M. Nappi. An end-to-end curriculum learning approach for autonomous driving scenarios. *IEEE Transactions on Intelligent Transportation Systems*, 23(10):19817–19826, 2022.
- [25] J. Schrittwieser, I. Antonoglou, T. Hubert, K. Simonyan, L. Sifre, S. Schmitt, A. Guez, E. Lockhart, D. Hassabis, T. Graepel, et al. Mastering atari, go, chess and shogi by planning with a learned model. *Nature*, 588(7839):604–609, 2020.
- [26] N. Hansen, H. Su, and X. Wang. Td-mpc2: Scalable, robust world models for continuous control. *arXiv preprint arXiv:2310.16828*, 2023.
- [27] I. Uchendu, T. Xiao, Y. Lu, B. Zhu, M. Yan, J. Simon, M. Bennice, C. Fu, C. Ma, J. Jiao, et al. Jump-start reinforcement learning. In *International Conference on Machine Learning*, pages 34556–34583. PMLR, 2023.
- [28] I. Kostrikov, A. Nair, and S. Levine. Offline reinforcement learning with implicit q-learning. *arXiv preprint arXiv:2110.06169*, 2021.
- [29] J. Li, C. Tang, M. Tomizuka, and W. Zhan. Dealing with the unknown: Pessimistic offline reinforcement learning. In *Conference on Robot Learning*, pages 1455–1464. PMLR, 2022.
- [30] A. Nair, A. Gupta, M. Dalal, and S. Levine. Awac: Accelerating online reinforcement learning with offline datasets. *arXiv preprint arXiv:2006.09359*, 2020.
- [31] M. Janner, Y. Du, J. B. Tenenbaum, and S. Levine. Planning with diffusion for flexible behavior synthesis. *arXiv preprint arXiv:2205.09991*, 2022.

- [32] C. Chi, S. Feng, Y. Du, Z. Xu, E. Cousineau, B. Burchfiel, and S. Song. Diffusion policy: Visuomotor policy learning via action diffusion. *arXiv preprint arXiv:2303.04137*, 2023.
- [33] P. Hansen-Estruch, I. Kostrikov, M. Janner, J. G. Kuba, and S. Levine. Idql: Implicit q-learning as an actor-critic method with diffusion policies. *arXiv preprint arXiv:2304.10573*, 2023.
- [34] V. Micheli, E. Alonso, and F. Fleuret. Transformers are sample-efficient world models. *arXiv preprint arXiv:2209.00588*, 2022.
- [35] Z. Gao, Y. Mu, C. Chen, J. Duan, P. Luo, Y. Lu, and S. E. Li. Enhance sample efficiency and robustness of end-to-end urban autonomous driving via semantic masked world model. *IEEE Transactions on Intelligent Transportation Systems*, 2024.
- [36] Y. Qu, H. Chu, S. Gao, J. Guan, H. Yan, L. Xiao, S. E. Li, and J. Duan. Rl-driven mppi: Accelerating online control laws calculation with offline policy. *IEEE Transactions on Intelligent Vehicles*, 9(2):3605–3616, 2024. doi:10.1109/TIV.2023.3348134.
- [37] A. Raffin, A. Hill, A. Gleave, A. Kanervisto, M. Ernestus, and N. Dormann. Stable-baselines3: Reliable reinforcement learning implementations. *Journal of Machine Learning Research*, 22 (268):1–8, 2021.
- [38] T. Silver, K. Allen, J. Tenenbaum, and L. Kaelbling. Residual policy learning. *arXiv preprint arXiv:1812.06298*, 2018.

## A Derivation

In this section, we provide a detailed proof of Theorem 1. We start with introducing a lemma to expand the action distribution  $q^*(U)$ .

**Lemma 1.** *Given an MDP defined by  $\mathcal{M} = (\mathcal{X}, \mathcal{U}, r, p)$ , with a deterministic state transition  $p$  defined with respect to a dynamics model  $F$ , the distribution of the action sequence  $q^*(U)$  at state  $\mathbf{x}_0$  in horizon  $T$ , where each action  $\mathbf{u}_t, t = 0, \dots, T-1$  is sequentially sampled from the maximum-entropy policy [19] is*

$$q^*(U) = \prod_{t=0}^{T-1} \pi^*(\mathbf{u}_t | \mathbf{x}_t). \quad (7)$$

*Proof.* Let  $\pi^*(\mathbf{u}_0, \mathbf{u}_1, \dots, \mathbf{u}_{T-1} | \mathbf{x}_0)$  denote the expanded notation of  $q^*(U)$  by substituting  $u_t$  and maximum-entropy policy  $\pi^*$ . Firstly, we apply the conditional probability formula to expand the equation:

$$\pi^*(\mathbf{u}_0, \mathbf{u}_1, \dots, \mathbf{u}_{T-1} | \mathbf{x}_0) = \pi^*(\mathbf{u}_0 | \mathbf{x}_0) \int_{\mathcal{X}} \pi^*(\mathbf{u}_1, \dots, \mathbf{u}_{T-1} | \mathbf{x}_0, \mathbf{u}_0, \mathbf{x}'_1) p(\mathbf{x}'_1 | \mathbf{x}_0, \mathbf{u}_0) d\mathbf{x}'_1. \quad (8)$$

Considering the Markov property of the problem,

$$\pi^*(\mathbf{u}_k, \dots, \mathbf{u}_{k+N} | \mathbf{x}_0, \mathbf{x}'_1, \dots, \mathbf{x}'_{k-1}, \mathbf{u}_0, \mathbf{u}_{k-1}, \mathbf{x}'_k) = \pi^*(\mathbf{u}_k, \dots, \mathbf{u}_{k+N} | \mathbf{x}'_k), \quad (9)$$

Eq. (8) could be further expanded recursively till the end:

$$\begin{aligned} \pi^*(\mathbf{u}_0, \mathbf{u}_1, \dots, \mathbf{u}_{T-1} | \mathbf{x}_0) &= \pi^*(\mathbf{u}_0 | \mathbf{x}_0) \int_{\mathcal{X}} \pi^*(\mathbf{u}_1, \dots, \mathbf{u}_{T-1} | \mathbf{x}_0, \mathbf{u}_0, \mathbf{x}'_1) p(\mathbf{x}'_1 | \mathbf{x}_0, \mathbf{u}_0) d\mathbf{x}'_1 \\ &= \pi^*(\mathbf{u}_0 | \mathbf{x}_0) \int_{\mathcal{X}} \pi^*(\mathbf{u}_1, \dots, \mathbf{u}_{T-1} | \mathbf{x}'_1) p(\mathbf{x}'_1 | \mathbf{x}_0, \mathbf{u}_0) d\mathbf{x}'_1 \\ &= \pi^*(\mathbf{u}_0 | \mathbf{x}_0) \int_{\mathcal{X}} \pi^*(\mathbf{u}_1 | \mathbf{x}'_1) p(\mathbf{x}'_1 | \mathbf{x}_0, \mathbf{u}_0) \\ &\quad \int_{\mathcal{X}} \pi^*(\mathbf{u}_2, \dots, \mathbf{u}_{T-1} | \mathbf{x}'_1) p(\mathbf{x}'_2 | \mathbf{x}'_1, \mathbf{u}_1) d\mathbf{x}'_1 d\mathbf{x}'_2 \\ &= \dots \\ &= \pi^*(\mathbf{u}_0 | \mathbf{x}_0) \int_{\mathcal{X}} p(\mathbf{x}'_1 | \mathbf{x}_0, \mathbf{u}_0) \pi^*(\mathbf{u}_1 | \mathbf{x}'_1) \\ &\quad \int \dots \int_{\mathcal{X}} \prod_{t=2}^{T-1} \pi^*(\mathbf{u}_t | \mathbf{x}'_t) p(\mathbf{x}'_t | \mathbf{x}'_{t-1}, \mathbf{u}_{t-1}) d\mathbf{x}'_1 \dots d\mathbf{x}'_{T-1}. \end{aligned} \quad (10)$$

Since the state transition  $p$  is a deterministic function

$$p(\mathbf{x}'_{t+1} | \mathbf{x}_t, \mathbf{u}_t) = \delta(\mathbf{x}'_{t+1}, F(\mathbf{x}_t, \mathbf{u}_t)), \quad (11)$$

the integral signs could be eliminated by defining  $\mathbf{x}_{t+1} = F(\mathbf{x}_t, \mathbf{u}_t)$ :

$$\begin{aligned}
\pi^*(\mathbf{u}_0, \mathbf{u}_1, \dots, \mathbf{u}_{T-1} | \mathbf{x}_0) &= \pi^*(\mathbf{u}_0 | \mathbf{x}_0) \int_{\mathcal{X}} p(\mathbf{x}'_1 | \mathbf{x}_0, \mathbf{u}_0) \pi^*(\mathbf{u}_1 | \mathbf{x}'_1) \\
&\quad \int \cdots \int_{\mathcal{X}} \prod_{t=2}^{T-1} \pi^*(\mathbf{u}_t | \mathbf{x}'_t) p(\mathbf{x}'_t | \mathbf{x}'_{t-1}, \mathbf{u}_{t-1}) d\mathbf{x}'_1 \cdots d\mathbf{x}'_{T-1} \\
&= \pi^*(\mathbf{u}_0 | \mathbf{x}_0) \int_{\mathcal{X}} \delta(\mathbf{x}'_{t+1}, F(\mathbf{x}_t, \mathbf{u}_t)) \pi^*(\mathbf{u}_1 | \mathbf{x}'_1) \\
&\quad \int \cdots \int_{\mathcal{X}} \prod_{t=2}^{T-1} \pi^*(\mathbf{u}_t | \mathbf{x}'_t) p(\mathbf{x}'_t | \mathbf{x}'_{t-1}, \mathbf{u}_{t-1}) d\mathbf{x}'_1 \cdots d\mathbf{x}'_{T-1} \quad (12) \\
&= \pi^*(\mathbf{u}_0 | \mathbf{x}_0) \pi^*(\mathbf{u}_1 | \mathbf{x}_1) \int_{\mathcal{X}} p(\mathbf{x}'_2 | \mathbf{x}_1, \mathbf{u}_1) \pi^*(\mathbf{u}_2 | \mathbf{x}'_2) \\
&\quad \int \cdots \int_{\mathcal{X}} \prod_{t=3}^{T-1} \pi^*(\mathbf{u}_t | \mathbf{x}'_t) p(\mathbf{x}'_t | \mathbf{x}'_{t-1}, \mathbf{u}_{t-1}) d\mathbf{x}'_2 \cdots d\mathbf{x}'_{T-1} \\
&= \cdots \\
&= \prod_{t=0}^{T-1} \pi^*(\mathbf{u}_t | \mathbf{x}_t).
\end{aligned}$$

QED

With Lemma 1, now we provide a detailed proof of Theorem 1.

**Theorem 1.** *Given an MDP defined by  $\mathcal{M} = (\mathcal{X}, \mathcal{U}, r, p)$ , with a deterministic state transition  $p$  defined with respect to a dynamics model  $F$  and a discount factor  $\gamma = 1$ , the distribution of the action sequence  $q^*(U)$  at state  $\mathbf{x}_0$  in horizon  $T$ , where each action  $\mathbf{u}_t, t = 0, \dots, T-1$  is sequentially sampled from the maximum-entropy policy [19] with an entropy weight  $\alpha$  is*

$$q^*(U) = \frac{1}{Z_{\mathbf{x}_0}} \exp \left( \frac{1}{\alpha} \left( \sum_{t=0}^{T-1} r(\mathbf{x}_t, \mathbf{u}_t) + V^*(\mathbf{x}_T) \right) \right), \quad (13)$$

where  $V^*$  is the soft value function [19] and  $\mathbf{x}_t$  is defined recursively from  $\mathbf{x}_0$  and  $U$  through the dynamics model  $F$  as  $\mathbf{x}_{t+1} = F(\mathbf{x}_t, \mathbf{u}_t), t = 0, \dots, T-1$ .

*Proof.* The maximum-entropy policy with an entropy weight  $\alpha$  solves the problem  $\mathcal{M}$  following the Boltzmann distribution:

$$\pi^*(\mathbf{u}_t | \mathbf{x}_t) = \frac{1}{Z_{\mathbf{x}_t}} \exp \left( \frac{1}{\alpha} Q^*(\mathbf{x}_t, \mathbf{u}_t) \right), \quad (14)$$

where  $Z_{\mathbf{x}_t}$  is the normalization factor defined as  $\int_{\mathcal{U}} \exp \left( \frac{1}{\alpha} Q^*(\mathbf{x}_t, \mathbf{u}_t) \right) d\mathbf{u}_t$  and  $Q^*(\mathbf{x}_t, \mathbf{u}_t)$  is the soft Q-function as defined in [19]:

$$Q^*(\mathbf{x}_t, \mathbf{u}_t) = r(\mathbf{x}_t, \mathbf{u}_t) + \alpha \log \int_{\mathcal{U}} \exp \left( \frac{1}{\alpha} Q^*(\mathbf{x}_{t+1}, \mathbf{u}_{t+1}) \right) d\mathbf{u}. \quad (15)$$

With Lemma 1, the optimal action distribution could be rewritten as:

$$q^*(U) = \prod_{t=0}^{T-1} \pi^*(\mathbf{u}_t | \mathbf{x}_t) \quad (16)$$

where each  $\mathbf{x}_t$  is defined recursively from  $\mathbf{x}_0$  and  $U$  through the dynamics model  $F$  as  $\mathbf{x}_{t+1} = F(\mathbf{x}_t, \mathbf{u}_t), t = 0, \dots, T-1$ . By substituting Eq. (14) and Eq. (15), Eq. (16) could be further expanded:

$$q^*(U) \tag{17a}$$

$$= \frac{1}{\prod_{t=0}^{T-1} Z_{\mathbf{x}_t}} \exp \left( \frac{1}{\alpha} \sum_{t=0}^{T-1} Q^*(\mathbf{x}_t, \mathbf{u}_t) \right) \tag{17b}$$

$$= \frac{1}{\prod_{t=0}^{T-1} Z_{\mathbf{x}_t}} \exp \left( \frac{1}{\alpha} \sum_{t=0}^{T-1} \left( r(\mathbf{x}_t, \mathbf{u}_t) + \alpha \log \int_{\mathcal{U}} \exp \left( \frac{1}{\alpha} Q^*(\mathbf{x}_{t+1}, \mathbf{u}_{t+1}) \right) d\mathbf{u} \right) \right) \tag{17c}$$

$$= \frac{1}{\prod_{t=0}^{T-1} Z_{\mathbf{x}_t}} \exp \left( \frac{1}{\alpha} \sum_{t=0}^{T-1} r(\mathbf{x}_t, \mathbf{u}_t) + \log \left( \prod_{t=1}^{T-1} Z_{\mathbf{x}_t} \right) + \log Z_{\mathbf{x}_T} \right) \tag{17d}$$

$$= \frac{\prod_{t=1}^{T-1} Z_{\mathbf{x}_t}}{\prod_{t=0}^{T-1} Z_{\mathbf{x}_t}} \exp \left( \frac{1}{\alpha} \left( \sum_{t=0}^{T-1} r(\mathbf{x}_t, \mathbf{u}_t) + \alpha \log Z_{\mathbf{x}_T} \right) \right) \tag{17e}$$

$$= \frac{1}{Z_{\mathbf{x}_0}} \exp \left( \frac{1}{\alpha} \left( \sum_{t=0}^{T-1} r(\mathbf{x}_t, \mathbf{u}_t) + V^*(\mathbf{x}_T) \right) \right), \tag{17f}$$

where Eq. (17b) results from substituting Eq. (14) and Eq. (17c) results from substituting Eq. (15).

In Eq. (17f),  $V^*(\mathbf{x}_T) = \alpha \log Z_{\mathbf{x}_T}$  is the soft value function defined in [19] at the terminal step. Each  $\mathbf{x}_t$  is defined recursively from  $\mathbf{x}_0$  and  $U$  through the dynamics model  $F$  as  $\mathbf{x}_{t+1} = F(\mathbf{x}_t, \mathbf{u}_t)$ ,  $t = 0, \dots, T-1$ . QED

## B Implementation Details in MuJoCo

All the experiments were conducted on Ubuntu 22.04 with Intel Core i9-9920X CPU @ 3.50GHz × 24, NVIDIA GeForce RTX 2080 Ti, and 125 GB RAM.

### B.1 MuJoCo Environment Configuration

In this section, we introduce the detailed configurations of the selected environments, including the basic tasks, add-on tasks, and the corresponding rewards. The action and observation space of all the environments follow the default settings in `gym[mujoco]-v3`.

**Half Cheetah.** In the `HalfCheetah` environment, the basic goal is to apply torque on the joints to make the cheetah run forward (right) as fast as possible. The state and action space has 17 and 6 dimensions, and the action represents the torques applied between links.

The basic reward consists of two parts:

$$\begin{aligned} \text{Forward Reward} : r_{\text{forward}}(\mathbf{x}_t, \mathbf{u}_t) &= \frac{\Delta x}{\Delta t} \\ \text{Control Cost} : r_{\text{control}}(\mathbf{x}_t, \mathbf{u}_t) &= -0.1 \times \|\mathbf{u}_t\|_2^2 \end{aligned} \tag{18}$$

During policy customization, we demand an additional task that requires the cheetah to limit the angle of its hind leg. This customization goal is formulated as an add-on reward function defined as:

$$r_R(\mathbf{x}_t, \mathbf{u}_t) = -10 \times |\theta_{\text{hind leg}}| \tag{19}$$

**Hopper.** In the `Hopper` environment, the basic goal is to make the hopper move in the forward direction by applying torques on the three hinges connecting the four body parts. The state and action space has 11 and 3 dimensions, and the action represents the torques applied between links.

The basic reward consists of three parts:

$$\begin{aligned} \text{Alive Reward} : r_{\text{alive}} &= 1 \\ \text{Forward Reward} : r_{\text{forward}}(\mathbf{x}_t, \mathbf{u}_t) &= \frac{\Delta x}{\Delta t} \\ \text{Control Cost} : r_{\text{control}}(\mathbf{x}_t, \mathbf{u}_t) &= -0.001 \times \|\mathbf{u}_t\|_2^2 \end{aligned} \tag{20}$$

The episode will terminate if the z-coordinate of the hopper is lower than 0.7, or the angle of the top is no longer contained in the closed interval  $[-0.2, 0.2]$ , or an element of the rest state is no longer contained in the closed interval  $[-100, 100]$ .

During policy customization, we demand an additional task that requires the hopper to jump higher along the z-axis. This customization goal is formulated as an add-on reward function defined as:

$$r_R(\mathbf{x}_t, \mathbf{u}_t) = 10 \times (z - 1) \quad (21)$$

**Swimmer.** In the Swimmer environment, the basic goal is to move as fast as possible towards the right by applying torque on the rotors. The state and action space has 8 and 2 dimensions, and the action represents the torques applied between links.

The basic reward consists of two parts:

$$\begin{aligned} \text{Forward Reward : } r_{\text{forward}}(\mathbf{x}_t, \mathbf{u}_t) &= \frac{\Delta x}{\Delta t} \\ \text{Control Cost : } r_{\text{control}}(\mathbf{x}_t, \mathbf{u}_t) &= -0.0001 \times \|\mathbf{u}_t\|_2^2 \end{aligned} \quad (22)$$

During policy customization, we demand an additional task that requires the agent to limit the angle of its first rotor. This customization goal is formulated as an add-on reward function defined as:

$$r_R(\mathbf{x}_t, \mathbf{u}_t) = -1 \times |\theta_{\text{first rotor}}| \quad (23)$$

**Ant.** In the Ant environment, the basic goal is to coordinate the four legs to move in the forward (right) direction by applying torques on the eight hinges connecting the two links of each leg and the torso (nine parts and eight hinges). The state and action space has 27 and 8 dimensions, and the action represents the torques applied at the hinge joints.

The basic reward consists of three parts:

$$\begin{aligned} \text{Alive Reward : } r_{\text{alive}} &= 1 \\ \text{Forward Reward : } r_{\text{forward}}(\mathbf{x}_t, \mathbf{u}_t) &= \frac{\Delta x}{\Delta t} \\ \text{Control Cost : } r_{\text{control}}(\mathbf{x}_t, \mathbf{u}_t) &= -0.5 \times \|\mathbf{u}_t\|_2^2 \end{aligned} \quad (24)$$

The episode will terminate if the z-coordinate of the torso is not in the closed interval  $[0.2, 1]$ . During experiments, we set the upper bound to inf for both prior policy training and planning experiments as it benefits both performances.

During policy customization, we demand an additional task that requires the ant to move along the y-axis. This customization goal is formulated as an add-on reward function defined as:

$$r_R(\mathbf{x}_t, \mathbf{u}_t) = \frac{\Delta y}{\Delta t} \quad (25)$$

## B.2 RL Prior Policy Training

The prior policies were constructed using Soft Actor-Critic (SAC) with the StableBaseline3 [37] implementation. The training was conducted in parallel across 32 environments. The hyperparameters used for RL prior policies training are shown in Table 3. Since this parameter setting performed poorly in the Swimmer task, we used the official benchmark checkpoint of Swimmer from Stable-Baseline3. Note that the prior policies do not necessarily need to be synthesized using RL. We report the experiment results with GAIL prior policies in Appendix F.

## B.3 Offline Dynamics Training

The hyperparameters used for offline dynamics training are shown in Table 4.



Table 3: RL Prior Policy Training Hyperparameters

Hyperparameter	Value
Hidden Layers	(256, 256, 256)
Activation	<i>ReLU</i>
$\gamma$	0.9
Target Update Interval	50
Learning Rate	$1e-4$
Gradient Step	1
Training Frequency	1
Batch Size	128
Optimizer	<i>Adam</i>
Total Samples	6400000
Capacity	1000000
Sampling	<i>Uniform</i>

Table 4: MuJoCo Offline Dynamics Training Hyperparameters

Hyperparameter	Value
Hidden Layers	(256, 256, 256, 256)
Activation	<i>Mish</i>
learning rate	$1e-5$
Training Frequency	10
Optimizer	<i>Adam</i>
Batch Size	256
Horizon	8
$\gamma$	0.9
Total Samples	200000
Capacity	50000
Sampling	<i>Uniform</i>

## B.4 Planning Hyperparameters

The hyperparameters used for online planning are shown in Table 5. At each step, the planners computes the result based on the current observation. Only the first action of the computed action sequence is sent to the system.

Table 5: Planning Hyperparameter in MuJoCo Tasks

Hyperparameter	Half Cheetah	Ant	Swimmer	Hopper
Horizon	2	5	5	8
Samples	10000	5000	5000	10000
Noise std.	0.017	0.005	0.02	0.005
$\omega'$	$1e-7$	$1e-2$	$1e-4$	$2e-7$
$\gamma$	0.9	0.9	0.9	0.9
$\lambda$	$5e-5$	$5e-3$	$1e-4$	$1e-5$

## C Implementation Details in GTS

All the GTS experiments were conducted on PlayStation 5 (PS5) and Ubuntu 20.04 with 12th Gen Intel Core i9-12900F  $\times$  24, NVIDIA GeForce RTX 3090, and 126 GB RAM. GTS ran independently on PS5 with a fixed frequency of 60Hz. The communication protocol returned the observation and received the control input with a frequency of 10Hz.

### C.1 GTS Environment Configuration

The action and observation spaces follow the configuration of GT Sophy 1.0 [18]. The reward used for GT Sophy 1.0 training was a handcrafted linear combination of reward components computed on the transition between the previous and current states, which included course progress, off-course penalty, wall penalty, tire-slip penalty, passing bonus, any-collision penalty, rear-end penalty, and unsporting-collision penalty [18]. During policy customization, we demand an additional task that

requires the GT Sophy 1.0 to drive on course. This customization goal is formulated as an add-on reward function defined as:

$$r_R(\mathbf{x}_t, \mathbf{u}_t) = -1000000 \times \text{ReLU}(d_{\text{center}}^2 - 7.3^2), \quad (26)$$

where  $d_{\text{center}}$  is the distance from the vehicle to the course center.

## C.2 Dynamics Design

We employed three main techniques to help us get an accurate dynamics model.

**Historical Observations** To address the partially observable Markov decision processes (POMDP) nature of the problem, we included historical observations in the input to help the model capture the implicit information.

**Splitting State Space** We divided the state space into two parts: the *dynamic states* and *map information*. We adopted a neural network with an MLP architecture to predict the *dynamic states*. In each step, we utilized the trained model to predict the *dynamic states* and leveraged the known map to calculate the *map information* based on the *dynamic states*.

**Physical Prior** Some physical states in the *dynamic states*, such as wheel load and slip angle, are intrinsically difficult to predict due to the limited observation. To reduce the variance brought by these difficult states, two neural networks were utilized to predict them and other states independently.

Table 6 shows the hyperparameters used for training these two MLPs to predict *dynamic states*.

Table 6: GTS Offline Dynamics Training Hyperparameters

Hyperparameter	Value
History Length	8
Hidden Layers	(2048, 2048, 2048)
Activation	<i>Mish</i>
Learning Rate	$1e - 5$
Training Steps	200000
Training Frequency	5
Batch Size	256
Optimizer	<i>Adam</i>
Capacity	2000000
Sampling	<i>Uniform</i>

## C.3 Planning Hyperparameters

To stabilize the planning process, we further utilized another hyperparameter *topratio* to select limited action sequence candidates with top-tier accumulated reward. The hyperparameters used for online planning are shown in Table 7. At each step, the planners computed the result based on the current observation. Only the first action of the computed action sequence was sent to the system.

Table 7: Planning Hyperparameter in GTS

Hyperparameter	Horizon	Samples	Noise std.	Top Ratio	$\omega'$	$\gamma$	$\lambda$
Value	4	3000	0.035	0.002	3	0.8	0.5

## C.4 Residual-SAC Training

In addition to the Residual-SAC algorithm, we adopted the idea of residual policy learning [38] to learn a policy that corrects the action of GT Sophy 1.0 by outputting an additive action, in which the initial policy was set as GT Sophy 1.0. As proposed in the same paper, the weights of the last layer in the actor network were initiated to be zero. The randomly initialized critic was trained alone with a fixed actor first. And then, both networks were trained together. The pipeline was developed upon the official implementation of RQL [14]. The training hyperparameters are shown in Table 8.

Table 8: Residual-SAC Training Hyperparameters

Hyperparameter	Value
Hidden Layers	(2048, 2048, 2048)
Activation	<i>ReLU</i>
Learning Rate	$1e - 4$
Target Update Interval	50
Gradient Step	1
Training Frequency	1
Batch Size	256
Optimizer	<i>Adam</i>
$\gamma$	0.9
Total Samples	10000000
Capacity	1000000
Sampling	<i>Uniform</i>

## D Extended Related Works

In this section, we provide a detailed discussion of the related works.

**Model-based RL.** Many works focused on combining learning-based agents with classical planning methods to enhance performance, especially in various model-based RL approaches. MuZero [25] employs its learned Actor as the search policy during the MCTS process and utilizes the Critic as the terminal value at the search leaf nodes to reduce the depth of the required search; TD-MPC2 [26] follows a similar approach and extends it to continuous task by utilizing MPPI as the continuous planner. RL-driven MPPI [36] chooses the distributional soft actor-critic (DSAC) algorithm as the prior policy and also adopts the MPPI as the planner. However, those methods are mainly addressing the planning within the same task and has full reward information of it. As for policy customization, it requires jointly optimizing both the original task of the prior policy without access to the reward information and add-on tasks, which makes it unsolvable by these methods.

**Planning with Prior Policy.** Some work in the literature addresses the similar customization requirements of the pre-trained Prior policy. Efficient game-theoretic planning [22] tries to use a planner to construct human behavior within the pre-trained prediction. However, it considers modeling the human reward with hand-designed features, which introduces further bias and constrains the overall performance. Deep Imitative Model [10] aims to direct an imitative policy to arbitrary goals during online usage. It is formulated as a planning problem solved online to find the trajectory that maximizes its posterior likelihood conditioned on the goal. Compared to theirs, we formulate the additional requirements as rewards instead of goals, which are more flexible to specify. Residual-MCTS proposed in residual Q-learning [14] addresses customization tasks in a similar setting to ours. However, its discrete nature makes it difficult to extend to continuous and more complex tasks.

**RL Fine-tuning.** There have been numerous works considering on the topic of fine-tuning policies. Jump-Start RL [27] (JSRL) uses a pre-trained prior policy as the guiding policy to form a curriculum of starting states for the exploration policy. However, it still requires the complete reward information to construct the task. Advantage Weighted Actor Critic [30] (AWAC) combines sample-efficient dynamic programming with maximum likelihood policy updates to leverage large amounts of offline data for quickly performing online fine-tuning of RL policies. Nevertheless, like all these fine-tuning methods, it still requires additional training for each new customization goal, which contradicts the goal of flexible deployment in customization tasks.

## E Visualization

### E.1 MuJoCo Experiments

We visualize some representative running examples from the MuJoCo environment in Fig. 3. As shown in the plot, the customized policies achieved significant improvements over the prior policies in meeting the objectives of the add-on tasks.

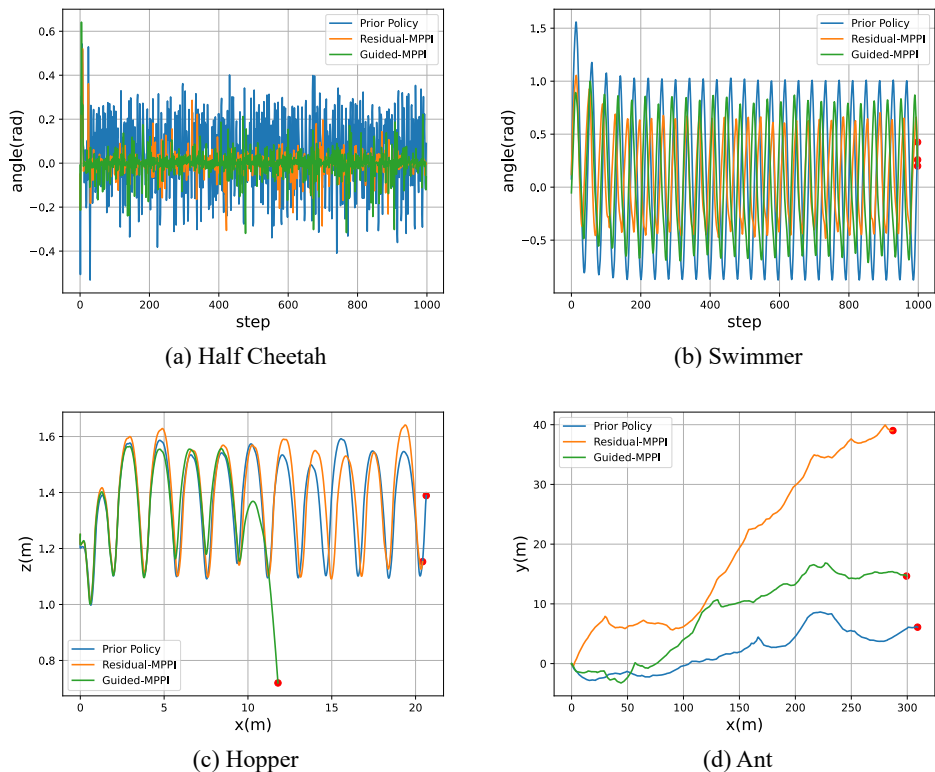


Figure 3: (a) The angle of the Half Cheetah’s hind leg vs. the environmental steps. (b) The angle of the Swimmer’s first rotor vs. the environmental steps. (c) The trajectory of the Hopper robot on the  $x$  and  $z$  axis.(d) The trajectory of the Ant robot on the  $x$  and  $y$  axis.

## E.2 GTS Experiments

We visualize the racing line selected by each policy at four typical corners to illustrate the differences among policies. As shown in Fig. 4, GT Sophy 1.0 exhibited aggressive racing lines that tend to be off course. Both Zero-shot MPPI and Few-shot MPPI were able to customize the behavior to drive more on the course, while the Few-shot MPPI chose a better racing line. In contrast, the Residual-SAC yields to an overly conservative behavior and keeps driving in the middle of the course.

We provide four typical complete trajectories of all policies in Fig. 5. Meanwhile, we visualize the difference between the actions selected by GT Sophy 1.0 and Residual-MPPI at each time step in Fig. 6. When driving at the corner, our method exerted notable influences on the prior policy, as shown in Fig. 6 (a). When driving at the straight, our method exerted minimal influences on the prior policy since most forward-predicted trajectories remain on course, as shown in Fig. 6 (b).

## F Additional Experimental Results

Residual-MPPI is applicable to any prior policies trained based on the maximum-entropy principle, not limited to RL methods. In this section, we conduct additional experiments upon the same MuJoCo environments with IL prior policies. The IL prior policies are obtained through Generative Adversarial Imitation Learning (GAIL) with expert data generated by the RL prior in the previous experiments. The hyperparameters used for training the IL prior policies are shown in Table 9, while the hyperparameters used for the learners are the same as the corresponding RL experts.

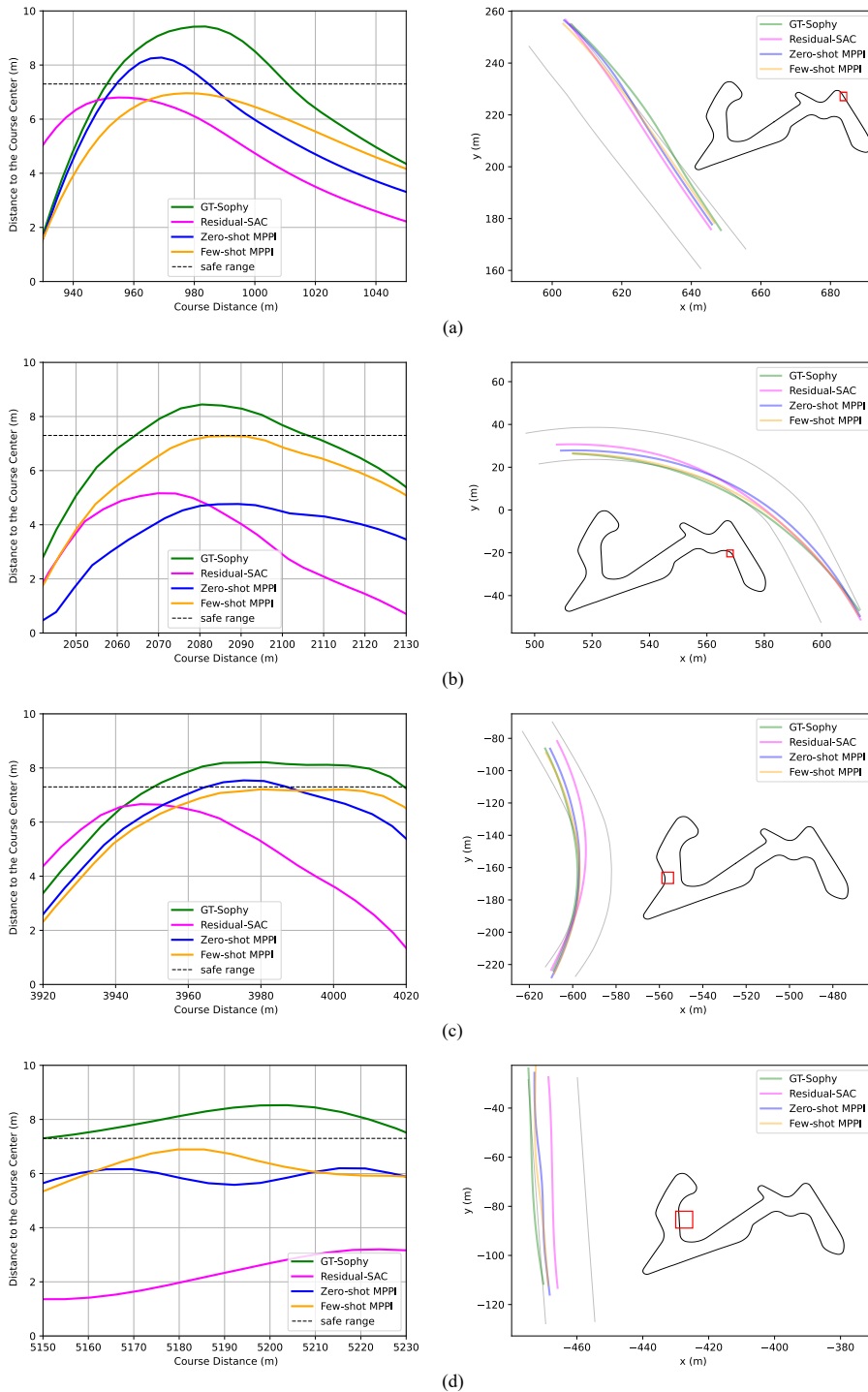


Figure 4: Route Selection Visualization at Different Cases. Different colors denote the different policies. In all cases, Residual-MPPI are able to customize the behavior to drive more on course. In (a) and (c), due to inaccurate dynamics, Zero-shot MPPI exhibits off-course behavior. In (b) and (d), although Few-shot MPPI and Zero-shot MPPI both drive on course, Few-shot MPPI tends to select a better route closer to the boundary with more accurate dynamics.

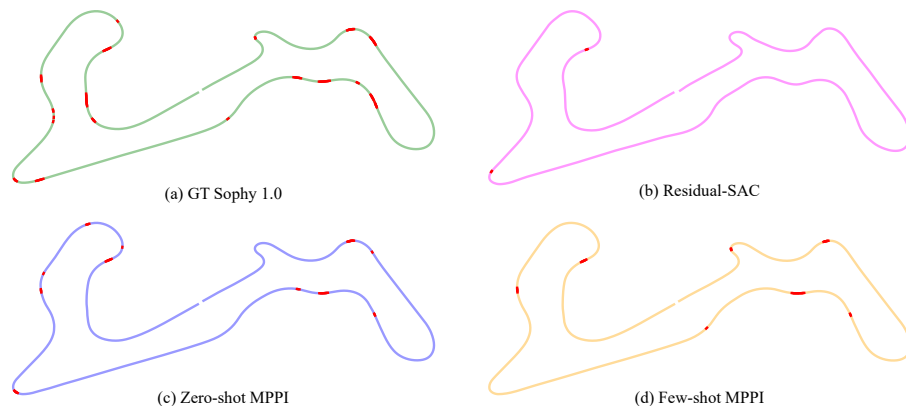


Figure 5: Typical complete trajectories of all policies. (a) The trajectory of GT Sophy 1.0. It finishes the lap in 117.762s with 93 steps off course. (b) The trajectory of Residual-SAC. It finishes the lap in 131.078s with 2 steps off course. (c) The trajectory of Zero-shot MPPI. It finishes the lap in 121.991s with 42 steps off course. (d) The trajectory of Few-shot MPPI. It finishes the lap in 120.542s with 34 steps off course.

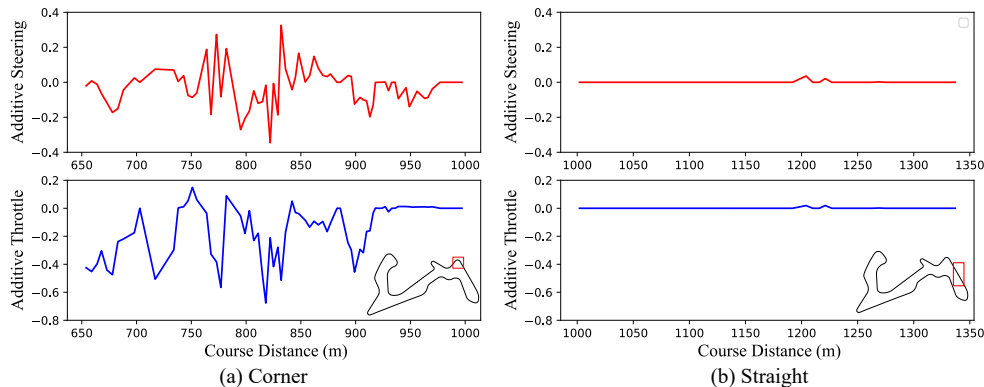


Figure 6: Additive Action of Residual-MPPI at Different Case. The additive throttle and steering are all linear normalized to  $-1$  to  $1$ .

Table 9: Hyperparameters of GAIL Imitated Polices

Hyperparameter	<i>Half Cheetah</i>	<i>Ant</i>	<i>Swimmer</i>	<i>Hopper</i>
expert_min_episodes	1000	100	1000	2000
demo_batch_size	512	25000	1024	1024
gen_replay_buffer_capacity	8192	50000	2048	2048
n_disc_updates_per_round	4	4	4	4

Table 10: Experimental Results of Zero-shot Residual-MPPI with IL Prior in MuJoCo

Env.	Policy	Full Task	Basic Task	Add-on Task	
		Total Reward	Basic Reward	$ \bar{\theta} $	Add-on Reward
Half Cheetah	Prior Policy	-935.10 ± 643.57	2322.33 ± 680.72	0.33 ± 0.01	-3257.43 ± 96.61
	Full-MPPI	-3612.30 ± 331.95	-1140.82 ± 169.74	0.25 ± 0.04	-2471.48 ± 395.98
	Guided-MPPI	-679.68 ± 236.98	2177.39 ± 271.87	0.29 ± 0.01	-2857.07 ± 124.82
	Residual-MPPI	<b>-405.97 ± 231.53</b>	2408.07 ± 197.93	<b>0.28 ± 0.01</b>	<b>-2814.04 ± 71.57</b>
Env.	Policy	Total Reward	Basic Reward	$ \bar{\theta} $	Add-on Reward
Swimmer	Prior Policy	-343.32 ± 3.18	329.63 ± 1.54	0.67 ± 0.00	-672.95 ± 1.86
	Full-MPPI	-1690.20 ± 101.46	12.48 ± 9.07	1.70 ± 0.10	-1702.67 ± 100.81
	Guided-MPPI	-122.06 ± 5.31	223.25 ± 4.83	0.35 ± 0.01	-345.31 ± 6.66
	Residual-MPPI	<b>-35.31 ± 7.19</b>	232.82 ± 3.95	<b>0.27 ± 0.01</b>	<b>-268.14 ± 7.93</b>
Env.	Policy	Total Reward	Basic Reward	$\bar{z}$	Add-on Reward
Hopper	Prior Policy	6786.03 ± 39.16	3438.86 ± 13.37	1.33 ± 0.00	3347.17 ± 27.67
	Full-MPPI	21.02 ± 3.07	3.73 ± 0.81	1.24 ± 0.00	17.29 ± 2.40
	Guided-MPPI	6720.80 ± 543.55	3393.86 ± 234.91	1.34 ± 0.01	3326.95 ± 313.20
	Residual-MPPI	<b>6850.97 ± 321.10</b>	3411.72 ± 133.23	<b>1.35 ± 0.01</b>	<b>3439.25 ± 188.67</b>
Env.	Policy	Total Reward	Basic Reward	$\bar{v}_y$	Add-on Reward
Ant	Prior Policy	4153.89 ± 1425.00	4770.24 ± 1595.86	-0.62 ± 0.22	-616.35 ± 224.59
	Full-MPPI	-2759.45 ± 179.90	-2760.16 ± 114.51	0.00 ± 0.11	0.71 ± 107.86
	Guided-MPPI	2792.82 ± 2158.99	2853.79 ± 2175.37	-0.06 ± 0.13	-60.97 ± 131.36
	Residual-MPPI	<b>5175.55 ± 1459.31</b>	4847.04 ± 1379.12	<b>0.33 ± 0.13</b>	<b>328.51 ± 132.60</b>

The evaluation results are computed over 500 episodes with all methods. The results are in the form of mean ± std.

The results are summarized in Table 10. Similar to the experiment results with the RL priors, the customized policies achieved significant improvements over the prior policies in meeting the objectives of the add-on tasks, which demonstrates the applicability of Residual-MPPI with IL priors.